JACS
JOURNAL OF THE AMERICAN CHEMICAL SOCIETY
Article
pubs.acs.org/JACS

Pt-Catalyzed C–C Activation Induced by C–H Activation

Miriam A. Bowring, Robert G. Bergman,* and T. Don Tilley*

Department of Chemistry, University of California, and Chemical Sciences Division, Lawrence Berkeley National Laboratory, Berkeley, California 94720, United States

Supporting Information

ABSTRACT: The catalytic cleavage of two C–C single bonds is achieved by treatment of the hydrocarbon substrate spiro[bicyclo[2.2.1]hept-2-ene-7,1′-cyclopropane] with Pt(II) catalysts such as $(Me_2bpy)PtPh(NTf_2)$ (Me_2bpy = 4,4′-dimethyl-2,2′-bipyridine, $NTf_2^- = N(SO_2CF_3)_2^-$). The surprising rearrangement product 1,2,4,7,7a-pentahydroindene is generated in good yield. The mechanism of C–C bond activation is investigated using NMR spectroscopy, electrospray ionization mass spectrometry, and deuterium labeling, along with density functional theory calculations. These studies support an unusual catalytic mechanism in which an initial masked C–H bond activation initiates successive C–C bond cleavage events.

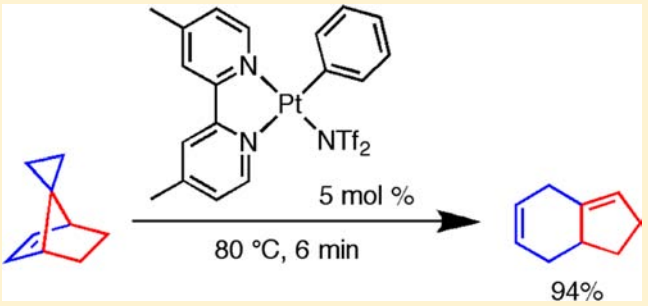

INTRODUCTION

C–H and C–C bond activations are potentially important chemical transformations with impacts in fundamental mechanistic chemistry and important synthetic applications.[1−9] 9 However, efficient homogeneous C–C activation reactions are not well developed and are far less common than those involving C–H bonds.[5−9] Generally, C–H bond activation reactions are used simply to install new functionality, but in several recent examples, they have been shown to initiate subsequent, more difficult bond activations.[10−12] Transformations that use C–H bond activation to initiate C–C bond activation in one overall conversion are especially rare.[11,12] The facilitation of catalytic C–C bond cleavage via C–H bond activation would provide a new approach to catalytic hydrocarbon transformations.

We report herein a new hydrocarbon rearrangement of a spirocyclopropane (**1**) to form a pentahydroindene (**2**), catalyzed by a platinum(II) complex (**3**) (eq 1). We

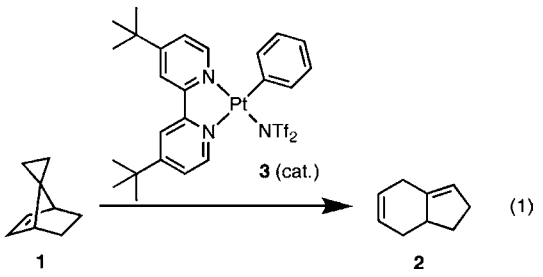

(1)

demonstrate that the likely mechanism includes a masked C–H activation event, which facilitates two C–C activation steps to generate the final rearrangement product. The use of C–H activation to initiate C–C bond cleavage in a catalytic cycle represents a remarkable new phenomenon, showing promise for generalized application to catalytic hydrocarbon conversions.

RESULTS AND DISCUSSION

Reaction Development. The bicyclic substrate spiro[bicyclo[2.2.1]hept-2-ene-7,1′-cyclopropane][13] (**1**) was originally envisioned as a mechanistic probe for hydrocarbon C–H activation catalysis (Scheme 1a). Previous reports have revealed the unexpected and crucial roles protons can play in reactions ostensibly catalyzed by transition-metal complexes.[14−16] Substrates designed to transform into divergent products depending on the mechanism of reaction have been effective in distinguishing between plausible reaction pathways.[16,17] We imagined that, in hydroarylation reactions, which can be either metal[18−20] or proton catalyzed,[14,21] bicyclic substrates such as **1** could provide crucial mechanistic information.

We expected that protonation of **1** would initiate a well-known Wagner–Meerwein carbocation rearrangement (Scheme 1a)[22] and that the spirocyclopropane moiety could accelerate this rearrangement by donating electron density to the developing neighboring carbocationic center in the transition state and serve as a label to break the degeneracy of the proposed carbocation rearrangement. The hydroarylation product resulting from nucleophilic attack of an arene on the rearranged carbocation would then be easily distinguishable from the product predicted for metal-catalyzed hydroarylation of **1** (Scheme 1a).

Substrate **1** was synthesized in three steps using a procedure adapted from Adam and co-workers (Scheme 2).[23] Cyclopentadiene was treated with base and 1,2-dichloroethane to give spiro[2.4]hepta-4,6-diene,[24] which then underwent a

Received: June 20, 2013
Published: August 20, 2013

   dx.doi.org/10.1021/ja406260j | J. Am. Chem. Soc. 2013, 135, 13121−13128

Scheme 1. Design of Substrate 1 as a Mechanistic Probe for Hydroarylation

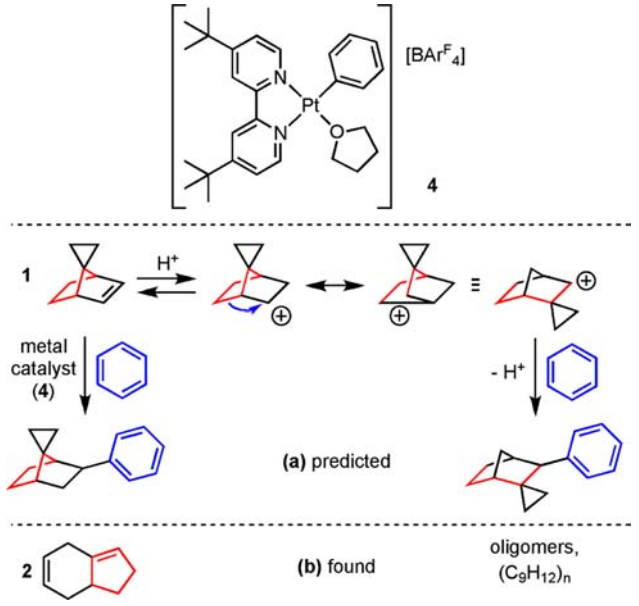

Scheme 2. Synthesis of Substrate 1

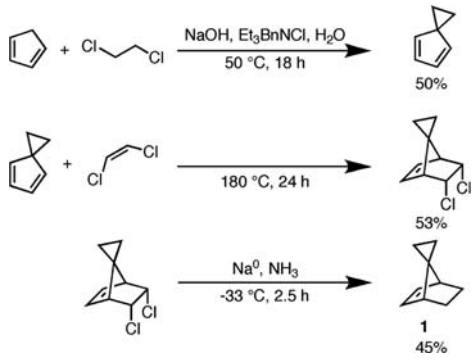

Diels–Alder reaction with *cis*-1,2-dichloroethylene.[25] The chlorine–carbon bonds were reductively cleaved with sodium in refluxing ammonia to give **1**.[23]

When subjected to three different catalysts for hydroarylation, substrate **1** proved to be a useful probe for in situ proton production by platinum catalysts as predicted, albeit with unexpected products (Scheme 1b). Compound **1** was stable in *o*-dichlorobenzene solution at 130 °C for four days in the absence of catalyst. When treated either with HOTf or with (^{t}Bu$_2$bpy)Pt(OTf)$_2$ (^{t}Bu$_2$bpy = 4,4′-di-*tert*-butyl-2,2′-bipyridine; OTf = SO_3CF_3), a platinum hydroarylation catalyst that was shown to rely on proton production, substrate **1** yielded similar product distributions.[14] Electrospray ionization mass spectrometry (ESI-MS) and ^{1}H NMR data for these products were consistent with oligomers[26] of **1** instead of the predicted hydroarylation product. In contrast, when treated with [Pt(^{t}Bu$_2$bpy)Ph(THF)][BAr$^F_4$] (Ar^F = 3,5-(CF$_3$)$_2$C$_6$H$_3$)) (**4**), a platinum hydroarylation catalyst that Gunnoe and co-workers showed does not rely on proton production,[18b,c] substrate **1** generated the surprising rearrangement product 1,2,4,7,7a-pentahydroindene (**2**) in 79% yield with no major side products. Substrate **1** thus exceeded its intended use as a mechanistic probe to differentiate hydroarylation mechanisms by also undergoing an unusual rearrangement reaction. The discovery of this rearrangement motivated a mechanistic study designed to uncover the new means of hydrocarbon activation that might be at play.

To develop a maximally efficient catalytic system for mechanistic investigations, the catalyst and reaction conditions were optimized. Catalyst **4** was of limited use for mechanistic study because of the counteranion. The BAr$^F_4{}^-$ counteranion was not inert, giving new resonances in the ^{19}F and ^{1}H NMR spectra during and after catalysis. In addition, the BAr$^F_4{}^-$ complex **4** was difficult to crystallize, hindering purification and crystallographic study of the catalyst and catalytic intermediates. Finally, Gunnoe and co-workers showed that a Lewis base such as THF or acetonitrile was necessary to stabilize the catalyst when BAr$^F_4{}^-$ was the counteranion.[18b,c] The equilibrium behavior of Lewis base coordination could both slow the reaction and complicate mechanistic investigations.

Use of the counteranion NTf$_2{}^-$ (NTf$_2{}^-$ = N(SO$_2$CF$_3$)$_2{}^-$)[27] instead of BAr$^F_4{}^-$ resulted in an improved catalyst for the rearrangement of **1** to **2**. The improved catalyst Pt(^{t}Bu$_2$bpy)-Ph(NTf$_2$) (**3**) was generated by protonolysis of one Pt–Ph bond of Pt(^{t}Bu$_2$bpy)Ph$_2$ by HNTf$_2$ (eq 2). The new complex

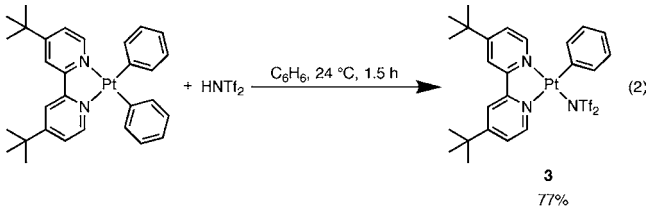

crystallized readily from toluene, and the X-ray crystal structure shows that the counteranion coordinates to the Pt center in the solid state (Figure 1). Furthermore, a resonance for the Pt-

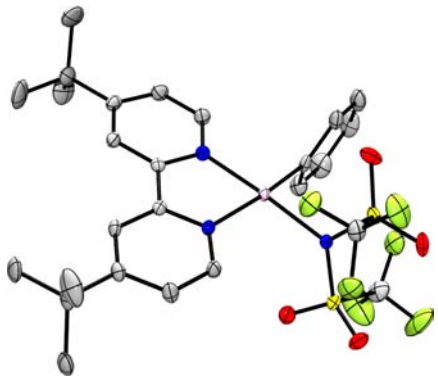

Figure 1. Molecular structure of **3** determined by single-crystal X-ray diffraction. The thermal ellipsoids are shown at the 50% probability level. Hydrogen atoms and toluene molecules are omitted for clarity.

bound NTf$_2{}^-$ counteranion was observed by ^{19}F NMR spectroscopy at −70 ppm in C$_6$D$_6$ solution. During and after the rearrangement reaction or upon displacement by an added Lewis base such as THF, the dissociated counteranion was observed (−78 ppm). No anion decomposition was observed by ^{19}F NMR spectroscopy after the catalytic rearrangement reaction to form **2** or after heating to 100 °C in a variety of solvents. The weakly coordinating counteranion eliminates the need for an additional Lewis base for stability.

The new catalyst **3** afforded faster and more efficient rearrangement of **1** than did the BAr$^F_4{}^-$ analogue **4** (Table 1,

dx.doi.org/10.1021/ja406260j | J. Am. Chem. Soc. 2013, 135, 13121–13128

Table 1. Catalysis Optimization: Effect of Catalyst Structure and Solvent on Yield

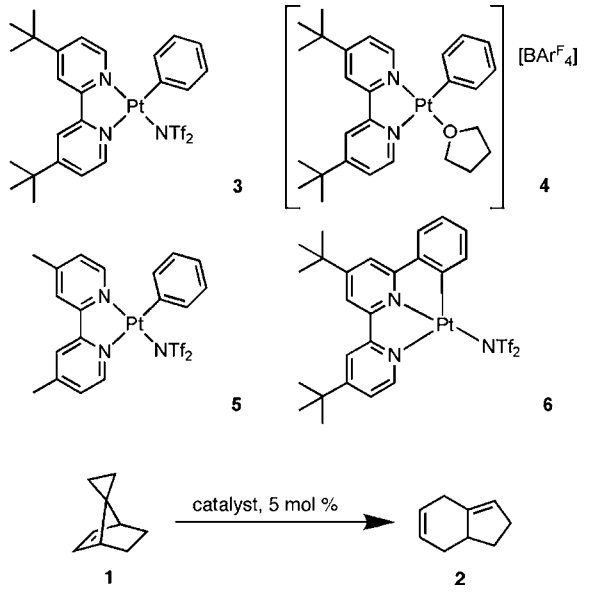

entry	catalyst	[1], mM	T, °C	solvent	time	yield[a] (%)
1	**4**	24	100	C_6D_6	18 days	46
2	**3**	24	100	C_6D_6	1.5 h	62
3	**3**	200	80	C_6D_6	1.5 h	67
4	**5**	200	80	C_6D_6	6.0 h	57
5	**5**	200	80	*o*-$C_6H_4F_2$	15 min	87
6	**5**	200	80	*o*-$C_6H_4Cl_2$	5.5 min	94
7	**5**	200	70	*o*-$C_6D_4Cl_2$	1.0 h	87
8	**5**	200	50	*o*-$C_6D_4Cl_2$	24 h	56
9	**6**	200	100	*o*-$C_6D_4Cl_2$	5 days	33

[a]Yields were determined by ^{1}H NMR spectroscopy integration relative to 1,3,5-tris(trifluoromethyl)benzene internal standard.

entries 1 and 2). At low concentration (24 mM) of substrate **1** in C_6D_6 at 100 °C with 5 mol % catalyst **4**, a 46% yield was observed after 18 days, while catalyst **3** generated a higher yield (62%) in 1.5 h.

Additional variants of the improved catalyst **3** were also synthesized for comparison. The catalyst Pt(Me$_2$bpy)Ph(NTf$_2$) (**5**) differs from **3** by a minor change in bipyridine substituents, from ^{t}Bu to Me (Me$_2$bpy = 4,4′-dimethyl-2,2′-bipyridine). Complexes **5** and **3** performed comparably as catalysts (Table 1, entries 3 and 4). At 80 °C in C_6D_6 with 5 mol % catalyst loading and 200 mM substrate **1**, 67% yield was reached after 1.5 h using catalyst **3** and 57% yield was reached after 6 h using catalyst **5**. A variant of **3** in which the phenyl group and bipyridine ligand are covalently tethered together, complex **6**, was also synthesized. Complex **6** was a catalyst for the rearrangement of **1** to **2**, but it was inefficient, requiring five days at 100 °C to reach 33% yield in *o*-dichlorobenzene-d_4 (Table 1, entry 9). Both of the efficient catalysts **3** and **5** were used for mechanistic investigations of the rearrangement reaction.

The activities of catalysts **3** and **5** were evaluated in several solvents. Coordinating and reactive solvents such as THF or CH_2Cl_2 were incompatible with the reaction, thwarting substrate conversion or causing catalyst decomposition, respectively. A comparison of benzene, *o*-difluorobenzene, and *o*-dichlorobenzene revealed that the highest catalyst activities were found in polar aromatic solvents (Table 1, entries 4–6). At 80 °C with 5 mol % catalyst **5**, 57% yield was reached after 6 h in benzene, but 87% yield was reached after 15 min in *o*-difluorobenzene, and the highest observed yield, 94%, was reached after 5.5 min in *o*-dichlorobenzene. The improved reactivity in polar aromatic solvents allowed the reaction temperature to be lowered further, resulting in final conditions optimized for ease of mechanistic study. The rearrangement product **2** was produced in 87% yield after 1 h at 70 °C in *o*-dichlorobenzene using catalyst **5** (Table 1, entry 7).

The initial discovery and optimization of the catalytic rearrangement reaction provide clues about its mechanism. The inability of HOTf to catalyze the rearrangement implies that the reaction is not acid catalyzed. (Simple Lewis acids including B(C_6F_5)$_3$ and $ZnCl_2$ also failed to catalyze the rearrangement.) The superiority of platinum catalysts lacking coordinated THF and the observation of anion dissociation during catalysis with **3** suggest that the open coordination site on platinum is essential to the transformation. The ability of complex **6**, bearing a tridentate form of the ligand set, to catalyze the rearrangement implies that only one open coordination site is necessary for the transformation and that the Ph group on catalysts **3** and **5** need not be eliminated during the reaction. The relative sluggishness of catalyst **6**, in which the phenyl group cannot rotate out of the bipyridine plane as it can in catalyst **3**, suggests that an out-of-plane geometry for the phenyl group is superior. Finally, the significant rate acceleration in more polar solvents indicates that a charge-separated state, such as anion dissociation to open a coordination site at platinum, is active during the transformation. Overall, these findings suggest that catalysis requires a single open coordination site at platinum.

Mechanistic Study. To examine the mechanism further, ^{1}H NMR spectroscopy was used to monitor the rearrangement under a variety of reaction conditions. Observation of an induction period, in which the rate of catalysis increases from a slow initial rate (Figure 2), suggests in situ homogeneous

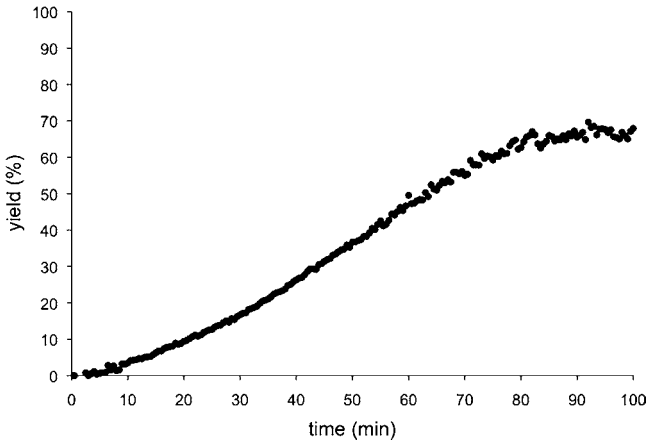

Figure 2. Induction period observed by ^{1}H NMR spectroscopy for rearrangement of **1** to **2**. Reaction conditions: 5 mol % catalyst **3**, 80 °C, C_6D_6.

catalyst generation (vide infra). The induction behavior is more pronounced for less polar solvents such as C_6D_6, supporting the notion that the activation step involves charge separation. Catalyst activation was further confirmed by observing the rearrangement of **1** to **2** using recycled catalyst that had been used for a previous run. In the case of this recycled catalyst, no

dx.doi.org/10.1021/ja406260j | J. Am. Chem. Soc. 2013, 135, 13121–13128

induction period was observed. Taken together, the observed induction period and activity of recycled catalyst further support the necessity of anion dissociation for catalysis and demonstrate that this dissociation takes the form of a kinetically relevant catalyst activation step.

Eventual deactivation of the catalyst was indicated by a slowing in the rate of reaction relative to simple first-order behavior. The catalyst deactivation was competitive enough with catalysis at lower reaction temperatures (50 °C) that the reaction failed to reach complete conversion. In these cases, activity was renewed upon addition of fresh catalyst. This renewal of catalytic activity in the presence of product **2** suggests that catalyst deactivation, rather than product inhibition, best explains the decreasing rate. While catalyst activation and deactivation prevent the extraction of simple rate laws from the kinetic data, they contribute to the development of a suitable mechanistic model.

The active and inactive forms of catalyst **5** were compared by ESI-MS characterization to identify catalytically active compounds. During active catalysis, a diluted aliquot of the crude catalytic mixture was collected and analyzed by ESI-MS (Figure 3a). After catalyst deactivation, a similarly prepared aliquot of the crude reaction mixture was also analyzed by ESI-MS (Figure 3b). Upon comparison, a single major peak present only during active catalysis was identified. On the basis of isotope distribution modeling, this peak (monoisotopic m/z = 575.20, Figure 3c) represents an adduct of the cationic portion of the catalyst, $(Me_2bpy)PtPh^+$, with the hydrocarbon substrate **1** or an isomer thereof (Figure 3d). The most abundant platinum complex observed after catalyst deactivation has a monoisotopic m/z value of 499.16, which is consistent with loss of a phenyl group relative to the active catalyst. This result implies that the phenyl group is necessary for catalysis. Thus, comparison of reaction mixtures containing active and inactive catalysts shows that the active catalytic species takes the straightforward form of a substrate-bound cationic Pt complex. Combined, these observations indicate that the rearrangement mechanism likely includes displacement of the triflimidate anion by the substrate, followed by rearrangement at the single open coordination site on platinum.

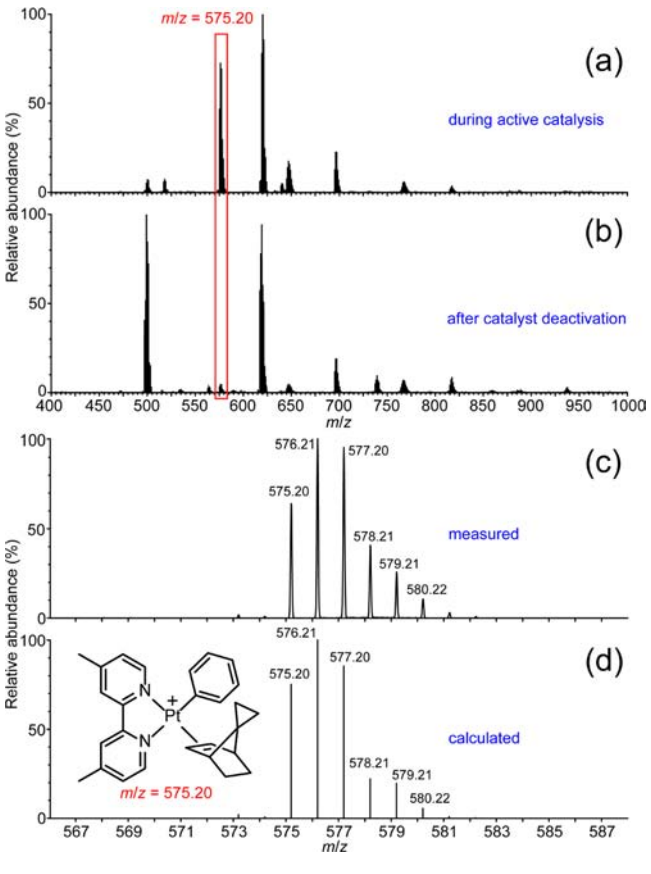

Figure 3. Isotopically resolved electrospray ionization mass spectra of reaction mixtures during active catalysis (a) and after catalyst deactivation (b). The highlighted peak was assigned as the cationic catalyst−substrate complex by comparison of the measured isotopic distribution (c) with the calculated natural-abundance isotopic distribution (d).

To probe the crucial rearrangement steps beyond substrate coordination and to overcome limitations imposed by the complex reaction kinetics, we designed a deuterium labeling experiment. Substrate **1**-d_4 was synthesized from 1,2-dichloroethane-d_4 by a route analogous to that for substrate **1**. When **1**-d_4 was subjected to the optimized rearrangement reaction conditions, product **2**-d_4 was produced in 89% yield with the quantitative regioselectivity and diastereoselectivity illustrated in eq 3.

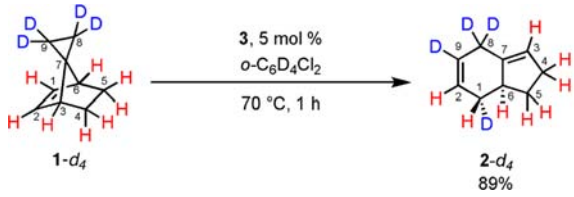

(3)

The selectivity of the reaction and the positions of the deuterium atoms in the product are instructive. The high selectivity rules out mechanistic possibilities that would result in scrambling, such as multiple reversible C−H activation, elimination, or protonation events. The positions of the deuterium atoms in the product are especially telling. The four deuterium atoms in the starting material **1**-d_4 constitute two adjacent methylene units (C8, C9). In the product, only one deuterated methylene unit remains, bound to a deuterated methine carbon. The fourth deuterium atom has undergone stereoselective migration across the molecule. The transfer of a deuterium to a third carbon atom in the formation of product **2**-d_4 indicates that C−D activation at one of the labeled positions is an essential step of the rearrangement. This C−D activation is a masked process, since the conversion of unlabeled starting material (**1**) to product (**2**) does not in itself necessitate C−H activation. The deuterium labeling study allowed the identification of C−H activation as a key step.

The deuterium labels also allow us to track the rearrangement of the carbon skeleton. Assuming that (a) the three deuterium atoms that occupy neighboring carbon atoms in the product do not participate in C−D activation and (b) the tertiary center and unlabeled pair of vicinal methylene units are conserved from reactant **1**-d_4 to product **2**-d_4, we can tentatively map the position of each carbon atom from the reactant to product (eq 3). This mapping indicates that three σ bonds (C9−D, C2−C3, and C7−C9) and one π bond (C1−C2) are broken. Two new σ bonds (C1−D and C2−C9) and two new π bonds (C2−C9 and C3−C7) are formed. The stereochemistry at C1 in the product **2**-d_4 indicates that the deuterium is transferred to the face of C1 that was *exo* in

dx.doi.org/10.1021/ja406260j | J. Am. Chem. Soc. 2013, 135, 13121−13128

starting material **1**-d_4. Thus, in addition to revealing the C−H activation step, the deuterium labeling study informs a putative carbon skeleton rearrangement map.

Our empirical mechanistic findings and the atom map developed from the deuterium labeling study facilitated the construction of a proposed mechanism for the transformation (Scheme 3). The catalyst initiation step, indicated by the

Scheme 3. Proposed Mechanism for the Catalytic Rearrangement of 1 to 2

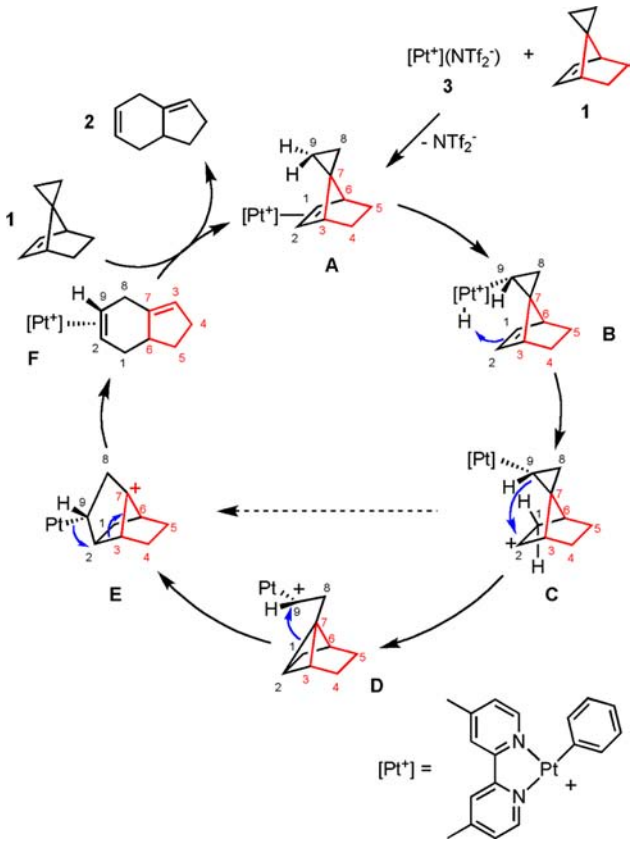

observed induction period, is likely the displacement of NTf_2^- by neutral substrate **1** at the platinum center to form the cationic platinum olefin complex **A**. The proposed first bond activation is C−H activation at C9, since C−H activation is known to be kinetically favored over C−C activation[9,28,29] and because initial C−C activation pathways would lead only to unproductive intermediates. C−H activation at C9 yields the cationic platinum(IV) alkyl hydride complex **B**. We propose that the acidic proton then transfers from the platinum center to the pendent olefin moiety, generating a carbocation, **C**. Intermediate **C** could undergo cyclopropane ring-opening to the carbocationic center, forming one of two rearranged carbocation structures, **D** or **E**. If intermediate **D**, in which the positive charge is stabilized α to the platinum center, is formed initially, an additional rearrangement step could then form the brexane-like[30] structure **E**. From intermediate **E**, only one bond, C2−C3, must break to form the product complex **F**. This could occur easily by elimination from platinum to introduce double bond character to the C9−C2 and C3−C7 bonds and formally restore the positive charge to the platinum center. Olefin exchange of product **2** by substrate **1** would then regenerate complex **A**, continuing the catalytic cycle. Derived directly from empirical findings, the proposed mechanism is consistent and plausible.

To evaluate any mechanistic proposal, it is essential to consider alternative pathways and to understand the basis for selectivity. Our best efforts yielded no productive alternative mechanistic hypotheses that were consistent with the experimental results. Most alternative pathways considered might lead reversibly to new organometallic complexes, but none feasibly form or release the observed organic product **2**. For example, initial C−C bond activation of the cyclopropane moiety would yield a metallocyclobutane, but further reactivity would not follow. A variety of C−C and C−H activations are likely to occur reversibly, but only intermediate **B** is poised for proton transfer and subsequent catalytic hydrocarbon rearrangement. Likewise, many nonproductive off-cycle intermediates may be formed reversibly throughout the transformation. For example, in the proposed mechanism (Scheme 3), intermediate **E** has the platinum atom and the C3 leaving group in an antiperiplanar conformation that allows elimination to occur to form **F**. If the stereochemistry at C9 is inverted at any point such that the platinum atom and C3 are not antiperiplanar in an intermediate such as **E**, no direct elimination of product can occur. Instead, equilibrium with the productive intermediate **E** will ultimately yield only the observed product **2**. Overall, the mechanism presented above is the only mechanism considered that could catalytically produce organic product **2**.

The possibility of heterogeneous catalysis was ruled out by a combination of mass spectrometry, variable-temperature studies, catalyst decomposition, and filtration. Positive-ion ESI-MS revealed no clusters containing more than one platinum atom during or after active catalysis. The reaction proceeded, albeit slowly, at room temperature (24 °C) and became inactive over time, both of which are atypical of nanoparticle formation. The active catalyst remained active when filtered through Celite, consistent with a homogeneous mechanism.

Density Functional Theory. The proposed mechanism is supported by density functional theory (DFT) studies (Figure 4). Gas-phase calculations demonstrated that each proposed intermediate **A** through **F** can exist at experimentally accessible energy levels. Transition-state calculations were performed, and appropriate transition states were identified for every elementary step, **A**−**B**, **B**−**C**, **C**−**D**, **D**−**E**, and **E**−**F**. Notably, no transition state that directly connected **C** to **E** could be identified, and this computational result supports inclusion of intermediate **D** in the proposed mechanism. The overall energy profile for the reaction (Figure 5) includes a relatively facile initial C−H activation (29 kcal/mol) and a barrierless (1 kcal/mol) final elimination from intermediate **E** to generate the product complex **F**. Between these two transition states lie three higher energy transition states, corresponding to proton transfer (38 kcal/mol relative to **A**) and two consecutive C−C bond cleavage events (36 kcal/mol relative to **A** in each case). The fact that every intermediate and transition state was located by calculation supports the proposed mechanism.

The calculated free energies exceed the value of 25 kcal/mol that is approximately consistent with the measured rates. Possible explanations for this discrepancy include general systematic errors found in DFT calculations and the inability of the calculations to account for direct solvent or counteranion involvement that may assist in the cationic rearrangement. Overall, the successful location by DFT of all proposed

dx.doi.org/10.1021/ja406260j | J. Am. Chem. Soc. 2013, 135, 13121−13128

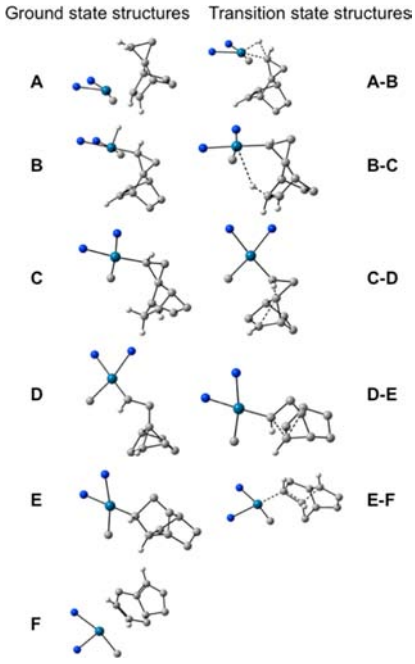

Figure 4. Calculated structures for all intermediates and transition states. Ligands are truncated for visual clarity, but calculations were run using the full ligand set present in catalyst **5**.

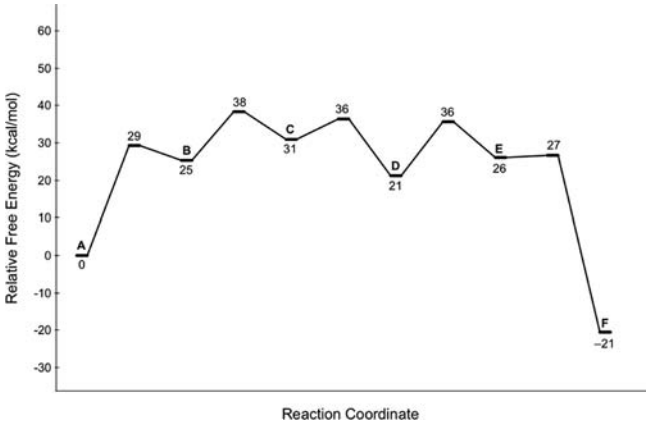

Figure 5. Reaction energy profile diagram.

intermediates and transition states at approximately reasonable energy levels supports the proposed catalytic mechanism in which C−H activation of substrate **1** occurs first and enables C−C bond activation.

CONCLUSION

In conclusion, we have discovered a new hydrocarbon rearrangement using platinum triflimidate precatalysts (**3**, **5**). On the basis of experimental results from NMR, mass spectrometry, and deuterium labeling studies, along with DFT calculations, we propose an unusual new mechanism for catalytic C−C bond activation. The proposed mechanism includes initial C−H activation of the substrate, which leads to subsequent carbocation generation and rearrangement to break two C−C bonds and catalytically release a bicyclic product. The reaction is noteworthy because it is a rare example of a catalytic C−C bond activation reaction and because it introduces an unprecedented mechanistic possibility: catalytic C−C bond cleavage driven by a masked C−H bond activation. We expect that catalytic systems can be designed to incorporate this feature, generating new means of activating and functionalizing hydrocarbons in a controlled, catalytic manner.

EXPERIMENTAL SECTION

General Considerations. All manipulations of air-sensitive compounds were conducted under a nitrogen atmosphere using standard Schlenk techniques or using a nitrogen atmosphere glovebox. Solvents were stored in poly(tetrafluoroethylene) (PTFE)-valved flasks after drying using Vacuum Atmospheres solvent purification systems or by distillation under nitrogen from appropriate drying agents. Deuterated solvents (Cambridge Isotopes) and 1,3,5-tris-(trifluoromethyl)benzene were dried over appropriate drying agents and vacuum-transferred prior to use. *cis*-5,6-Dichlorospiro[bicyclo-[2.2.1]hept[2]ene-7,1′-cyclopropane],[24,25] [Pt(^{t}Bu$_2$bpy)Ph(THF)]-[BAr$^F_4$] (**4**),[18c] Pt(^{t}Bu$_2$bpy)Ph$_2$,[31−33] PtPh$_2$(SMe$_2$)$_2$,[32] and Pt(κ^3-6-phenyl-4,4′-di-*tert*-butyl-2,2′-bipyridine)Cl[34] were prepared according to literature procedures. Ammonia (Scott Specialty Gases), 1,2-dichloroethane-d_4 (Cambridge Isotopes), and dicyclopentadiene, *cis*-1,2-dichloroethylene, sodium, phenyllithium, and AgNTf$_2$ (Aldrich) were purchased and used without further purification. HNTf$_2$ was purchased from Aldrich and sublimed before use. NMR spectra were recorded on Bruker spectrometers at room temperature unless otherwise noted. Spectra were referenced internally by the residual solvent proton signal for ^{1}H NMR, solvent signal for ^{13}C NMR, and 1,3,5-tris(trifluoromethyl)benzene signal for ^{19}F NMR experiments. X-ray analyses were carried out at the University of California, Berkeley, College of Chemistry X-ray Crystallography Facility. Measurements were made on an APEX charge-coupled device (CCD) area detector with Mo Kα radiation (λ = 0.71073 Å) monochromated with QUAZAR multilayer mirrors. Structures were solved using the SHELXTL (version 5.1) program library (G. Sheldrick, Bruker Analytical Systems, Madison, WI). All software and sources of scattering factors are contained in the SHELXTL (version 5.1) program library. Elemental analyses were performed by the University of California, Berkeley, College of Chemistry Microanalytical Facility. ESI-MS data were acquired in the QB3/College of Chemistry Mass Spectrometry Facility at the University of California, Berkeley, using a Waters (Milford, MA) Q-Tof Premier quadrupole time-of-flight mass spectrometer in the positive ion mode. Preparatory gas chromatography was carried out using a GOW-MAC series 400P basic isothermal gas chromatograph, DataApex Clarity Lite chromatography station software, and a custom-made PTFE-stoppered glass receiving vessel.

Synthesis of 1. The synthesis was adapted from the literature procedure[23] as follows: *cis*-5,6-Dichlorospiro[bicyclo[2.2.1]-hept[2]-ene-7,1′-cyclopropane] (2.00 g, 10.6 mmol) and sodium metal (3.20 g, 139 mmol) were put into a 250 mL round-bottom flask equipped with a glass-coated stir bar and both a bath and a condenser at −77 °C. Ammonia (150 mL) was condensed into the flask. The flask was allowed to warm to reflux temperature under N$_2$. After 2.5 h, the flask was cooled to −77 °C. Pristane (5 mL) was added, and then water (5 mL) was added slowly. The cold bath was removed, and ammonia was allowed to evaporate. The pristane layer was separated from the water layer and dried over magnesium sulfate. Compound **1** was separated from pristane by preparatory gas chromatography (sequential 0.4 mL injections, 8 ft × 1/4 in. Carbowax 20 column, column temperature 125 °C, detector and injection port temperatures 140 °C, collection vessel temperature −77 °C, UHP He carrier gas flow rate 100 mL/min, retention time 10 min) to give **1** as a clear, colorless liquid (45% yield, >95% pure by ^{1}H NMR).

Synthesis of 1-d_4. Compound **1**-d_4 was synthesized identically to **1**,[23−25] except for substitution of 1,2-dichloroethane-d_4 for 1,2-dichloroethane. ^{1}H NMR (*o*-dichlorobenzene-d_4, 400 MHz): δ 6.09 (m, 2H), 2.10 (m, 2H), 1.78 (m, 2H), 1.06 (m, 2H). ^{2}H NMR (*o*-dichlorobenzene-d_4, 400 MHz): δ 0.40 (s, 2D), 0.20 (s, 2D).

Representative Catalytic Procedure for Conversion of 1 to 2. A stock solution was prepared containing substrate **1** (260 mM) and 1,3,5-tris(trifluoromethyl)benzene (22 mM) as an internal standard. To a sample of catalyst **5** (2.2 mg, 3.0 μmol) was added the substrate

dx.doi.org/10.1021/ja406260j | J. Am. Chem. Soc. 2013, 135, 13121−13128

solution (230 μL, 60 μmol, of substrate **1**, 5 μmol of standard). The resulting clear yellow solution was transferred to a medium-walled PTFE-valved NMR tube. The tube was heated to 70 °C for 50 min. The yield of **2** (87%) was determined by ^{1}H NMR integration relative to the internal standard.

NMR Characterization of Product 2..[35,36] Product **2** was isolated by filtration of the catalytic mixture through a silica plug followed by preparatory gas chromatography (0.3 mL injection, 8 ft × 1/4 in. DC710 column, column temperature 135 °C, detector and injection port temperatures 150 °C, collection vessel temperature 0 °C, UHP He carrier gas flow rate 100 mL/min, retention time 30 min) to give **2** as a clear, colorless liquid. The following assignments were based on HSQC, COSY, and NOESY analyses. The abbreviation "ax" designates axial, or *trans* to C6−H, while "eq" represents equatorial, or *cis* to C6−H. The numbering of the carbon atoms is defined in eq 3. ^{1}H NMR ($CDCl_3$, 400 MHz): δ 5.74−5.67 (m, 1H, C2−H), 5.67−5.61 (m, 1H C9−H), 5.38 (m, 1H, C3−H), 2.85 (m, 2H, H−C8−H), 2.71−2.59 (m, 1H, C6−H), 2.44−2.23 (m, 3H, H−C4−H and C1−H_{eq}), 2.22−2.11 (m, 1H, C5−H_{eq}), 1.85−1.74 (m, 1H, C1−H_{ax}), 1.50−1.40 (m, 1H, C5−H_{ax}). ^{13}C NMR ($CDCl_3$, 400 MHz): δ 142.5 (C7), 127.1 (C2), 126.2 (C9), 121.3 (C3), 41.9 (C6), 34.7 (C1), 31.1 (C4), 30.4 (C5), 28.3 (C8).

NMR Characterization of Product 2-d_4. ^{1}H NMR (*o*-dichlorobenzene-d_4, 400 MHz): δ 5.65 (s, 1H, C2−H), 5.32−5.28 (m, 1H, C3−H), 2.64−2.56 (m, 1H, C6−H), 2.35−2.22 (m, 2H, H−C4−H), 2.16−2.07 (m, 1H, C5−H_{eq}), 1.76−1.69 (m, 1.85−1.74, C1−H_{ax}), 1.44−1.35 (m, 1H, C5−H_{ax}). ^{2}H NMR (*o*-dichlorobenzene-d_4, 400 MHz): δ 5.61 (m, 1D, C9−D), 3.79 (s, 2D, D−C8−D), 2.37−2.19 (m, 1D, C1−D_{eq}).

Synthesis of 3. Pt(^{t}Bu$_2$bpy)Ph$_2$ (40 mg, 64 μmol) was dissolved in a minimum of benzene (2 mL). To this dark orange solution was added a solution of $HNTf_2$ (17 mg, 60 μmol) in benzene (2 mL). The color changed to yellow. After 1.5 h, pentane was added (16 mL). The resulting yellow precipitate was collected on a frit, dried under vacuum, then dissolved in a minimum of toluene (20 mL), and cooled to −30 °C. After 44 h, product **4** was collected as yellow crystals and dried under vacuum (38 mg, 77% yield). Crystals suitable for X-ray diffraction were grown by cooling a solution of **4** (10 mg) in toluene (7 mL) to −30 °C for 18 h. Anal. Calcd for $C_{26}H_{29}F_6N_3O_4PtS_2{\cdot}C_7H_8$: C, 43.42; H, 4.09; N, 4.60. Found: C, 43.06; H, 4.27; N, 4.24. ^{1}H NMR (C_6D_6, 400 MHz): δ 9.16 (d, J = 6 Hz, 1H), 8.16 (d, J = 8 Hz, 2H), 7.87 (d, J = 6 Hz, J_{Pt-C} = 32 Hz, 1H), 7.35 (m, 3H), 7.07 (s, 1H), 6.94 (s, 1H), 6.68 (d, J = 6 Hz, 1H), 5.82 (d, J = 6 Hz, 1H), 0.88 (s, 9H), 0.79 (s, 9H). ^{19}F NMR (C_6D_6, 400 MHz): δ −70.3 (s, 6F). ^{13}C NMR (*o*-$C_6D_4Cl_2$, 600 MHz): δ 164.4, 164.2, 157.4, 153.8, 151.6, 148.7, 137.8, 124.5, 124.3, 123.9, 123.0, 120.8, 119.2, 119.0, 118.6, 35.6, 35.5, 30.1, 29.9.

Synthesis of Pt(Me$_2$bpy)Ph$_2$. To $PtPh_2(SMe_2)_2$ (1.1 g, 2.4 mmol) were added Me_2bpy (0.50 g, 2.7 mmol) and diethyl ether (150 mL). The suspension was stirred for 21 h, and Pt(Me_2bpy)Ph_2 was collected by filtration as a fine yellow powder, then washed with diethyl ether, and dried under vacuum (1.0 g, 77% yield). Anal. Calcd for $C_{24}H_{22}N_2Pt$: C, 54.03; H, 4.16; N, 5.25. Found: C, 53.64; H, 3.66; N, 5.03. ^{1}H NMR ($CDCl_3$, 500 MHz): δ 8.49 (d, J = 6 Hz, 2H), 7.86 (s, 2H), 7.56 (d, J = 7 Hz, J_{PtH} = 34 Hz, 4H), 7.18 (d, J = 6 Hz, 2H), 7.09 (t, J = 7, 4H), 6.96 (t, J = 7 Hz, 2H), 2.44 (s, 6H). ^{13}C NMR ($CDCl_3$, 500 MHz): δ 156.0, 150.0, 149.3, 145.5, 138.5, 127.7, 127.2, 122.8, 121.9, 21.9.

Synthesis of 5. To a suspension of Pt(Me_2bpy)Ph_2 (34 mg, 64 μmol) in benzene (12 mL) was added a solution of $HNTf_2$ (17 mg, 60 μmol) in benzene (3 mL). The color changed from dark to light yellow. After 1 h of stirring, the solvent volume was reduced to 5 mL under vacuum, and pentane was added (10 mL). The resulting yellow precipitate was collected on a frit, then rinsed with a 1:2 benzene/pentane mixture (5 × 3 mL), and dried under vacuum (34 mg, 77% yield). Anal. Calcd for $C_{20}H_{17}F_6N_3O_4PtS_2$: C, 32.61; H, 2.33; N, 5.70; S, 8.71. Found: C, 33.32; H, 2.40; N, 5.54; S, 9.10. ^{1}H NMR (C_6D_6, 400 MHz): δ 8.96 (d, J = 6 Hz, 1H), 8.08 (d, J = 7 Hz, 2H), 7.98 (d, J = 6 Hz, J_{Pt-C} = 31.4, 1H), 7.30 (m, 3H), 6.59 (s, 1H), 6.46 (s, 1H), 6.16 (d, J = 6 Hz, 1H), 5.53 (d, J = 6 Hz, 1H), 1.62 (s, 3H), 1.45 (s, 3H). ^{13}C NMR (*o*-$C_6D_4Cl_2$, 600 MHz): δ 156.9, 153.5, 151.8, 151.6, 151.1, 148.1, 137.8, 136.3, 135.0, 125.6, 124.4, 123.3, 122.9, 120.8, 118.6, 21.6, 21.5. ^{19}F NMR (C_6D_6, 400 MHz): δ −70.3 (s, 6F).

Synthesis of 6. To $AgNTf_2$ (39 mg, 100 μmol) was added a solution of Pt(κ^3-6-phenyl-4,4′-di-*tert*-butyl-2,2′-bipyridine)Cl (57 mg, 100 μmol) in *o*-dichlorobenzene (5 mL). The clear red solution was stirred in the dark for three days. A gray precipitate formed, which was removed by filtration through Celite. Pentane (30 mL) was added to the filtrate. The resulting yellow precipitate was collected on a frit, washed with pentane (8 × 2 mL), and then dried under vacuum (66 mg, 81% yield). Crystals suitable for X-ray diffraction were obtained from benzene at 24 °C after three days. Anal. Calcd for $C_{26}H_{27}F_6N_3O_4PtS_4$: C, 38.14; H, 3.32; N, 5.13; S, 7.83. Found: C, 37.88; H, 3.17; N, 4.94; S, 8.09. ^{1}H NMR (*o*-$C_6D_4Cl_2$, 500 MHz): δ 8.70 (d, J = 5.5, 1H), 7.70 (s, 1H), 7.64 (d, J = 7.61, 1H), 7.40 (s, 1H), 7.36 (s, 1H), 7.34 (m, 1H), 7.30 (d, J = 7.8, 1H), 7.24 (m, 1H), 7.06 (m, 1H), 1.38 (s, 9H), 1.26 (s, 9H). ^{13}C NMR (*o*-$C_6D_4Cl_2$, 600 MHz): δ 167.3, 165.7, 165.2, 156.2, 154.7, 150.1, 146.8, 136.0, 131.1, 125.0 (br), 124.6, 124.4, 121.1, 119.5, 118.9, 115.8, 114.7, 36.0, 35.6, 30.4, 30.1. ^{19}F NMR (C_6D_6, 400 MHz): δ −73.1 (s, 6F).

Computational Details. All calculations were performed using the Gaussian '09 suite of programs[37] in the Molecular Graphics and Computing Facility of the College of Chemistry, University of California, Berkeley. The crystallographically determined atomic coordinates of **4** were used as starting points for gas-phase geometry optimization calculations for catalyst **5** and its derivatives, after transformation of ^{t}Bu groups into Me groups. The B3LYP hybrid functional was used with the 6-31G(d,p) basis set for all main-group elements and the SDD basis set for platinum. Stationary points were confirmed by frequency calculations, showing all positive vibrations for minima and one imaginary vibration for transition states. Frequency calculations were carried out at 298.15 K and 1 atm. Molecular images were rendered and exported from Gaussview. Transition-state structures were located using a combination of relaxed coordinate scans and geometry optimizations, and they were all confirmed by intrinsic reaction coordinate calculations or by geometry minimization after perturbation of the transition-state structure along the imaginary vibrational mode. Calculations for key steps were repeated with either solvent corrections (*o*-dichlorobenzene, benzene) or an alternate functional (ωB97XD), and the results were similar to those from the original calculations.

■ ASSOCIATED CONTENT

Ⓢ Supporting Information

Additional experimental information, NMR characterization details for **1**-d_4 and **2**-d_4, and X-ray crystallographic details and CIF files for **3** and **6**. This material is available free of charge via the Internet at http://pubs.acs.org.

■ AUTHOR INFORMATION

Corresponding Author

rbergman@berkeley.edu; tdtilley@berkeley.edu

Notes

The authors declare no competing financial interest.

■ ACKNOWLEDGMENTS

We gratefully acknowledge financial support from the Director of the Office of Energy Research, Office of Basic Energy Sciences, Chemical Sciences Division, of the U.S. Department of Energy under Contract DE-AC02-05CH11231. For the synthesis of starting materials, we thank Kathryn Liu. For technical assistance and helpful discussion, we thank Dr. Kathleen A. Durkin and Dr. Xinzheng Yang of the College of Chemistry Molecular Graphics and Computation Facility, Dr. Anthony T. Iavarone of the QB3/Chemistry Mass Spectrometry Facility, and Dr. Antonio DiPasquale of the College of

Chemistry X-ray Crystallography Facility, all at the University of California, Berkeley.

REFERENCES

(1) Crabtree, R. H., Ed. *Chem. Rev.* **2010**, *110*, 575 ("Selective Functionalization of C−H Bonds" special issue).
(2) Davies, H. M. L., Du Bois, J., Yu, J.-Q., Eds. *Chem. Soc. Rev.* **2011**, *40*, 1855 ("C−H Functionalisation in Organic Synthesis" special issue).
(3) Labinger, J. A.; Bercaw, J. E. *Nature* **2002**, *417*, 507.
(4) Bergman, R. G. *Nature* **2007**, *446*, 391.
(5) Representative reviews addressing catalytic C−C activation: (a) Aïssa, C. *Synthesis* **2011**, *21*, 3389. (b) Necas, D.; Kotora, M. *Curr. Org. Chem.* **2007**, *11*, 1566. (c) Rybtchinski, B.; Milstein, D. *Angew. Chem., Int. Ed.* **1999**, *38*, 870. (d) Murakami, M.; Ito, Y. *Topics in Organometallic Chemistry*; Springer: Berlin/Heidelberg, 1999; Vol. 3, p 97.
(6) (a) Pellissier, H. *Adv. Synth. Catal.* **2011**, *353*, 189. (b) Wender, P. A.; Takahashi, H.; Witulski, B. *J. Am. Chem. Soc.* **1995**, *117*, 4720.
(7) (a) Jennings, P. W.; Johnson, L. L. *Chem. Rev.* **1994**, *94*, 2241. (b) Hoberg, J. O.; Jennings, P. W. *J. Am. Chem. Soc.* **1990**, *112*, 5347.
(8) Mukai, C.; Ohta, Y.; Oura, Y.; Kawaguchi, Y.; Inagaki, F. *J. Am. Chem. Soc.* **2012**, *134*, 19580.
(9) Hartwig, J. F. *Organotransition Metal Chemistry*; University Science Books: Mill Valley, CA, 2010.
(10) (a) Kundu, S.; Choi, J.; Wang, D. Y.; Choliy, Y.; Emge, T. J.; Krogh-Jespersen, K.; Goldman, A. S. *J. Am. Chem. Soc.* **2013**, *135*, 5127. (b) Choi, J.; Wang, D. Y.; Kundu, S.; Choliy, Y.; Emge, T. J.; Krogh-Jespersen, K.; Goldman, A. S. *Science* **2011**, *332*, 1545. (c) Choi, J.; Choliy, Y.; Zhang, X.; Emge, T. J.; Krogh-Jespersen, K.; Goldman, A. S. *J. Am. Chem. Soc.* **2009**, *131*, 15627.
(11) (a) Aïssa, C.; Crépin, D.; Tetlow, D. J.; Ho, K. Y. T. *Org. Lett.* **2013**, *15*, 1322. (b) Crépin, D.; Tugny, C.; Murray, J. H.; Aïssa, C. *Chem. Commun.* **2011**, *47*, 10957. (c) Crépin, D.; Dawick, J.; Aïssa, C. *Angew. Chem., Int. Ed.* **2010**, *49*, 620. (d) Aïssa, C.; Fürstner, A. *J. Am. Chem. Soc.* **2007**, *129*, 14836. (e) Aloise, A. D.; Layton, M. E.; Shair, M. D. *J. Am. Chem. Soc.* **2000**, *122*, 12610.
(12) (a) Jiang, M.; Liu, L.-P.; Shi, M.; Li, Y. *Org. Lett.* **2009**, *12*, 116. (b) Shi, M.; Liu, L.-P.; Tang, J. *J. Am. Chem. Soc.* **2006**, *128*, 7430.
(13) Alder, K.; Ache, H.-J.; Flock, F. H. *Chem. Ber.* **1960**, *93*, 1888.
(14) Bowring, M. A.; Bergman, R. G.; Tilley, T. D. *Organometallics* **2011**, *30*, 1295.
(15) (a) Taylor, J. G.; Adrio, L. A.; Hii, K. K. *Dalton Trans.* **2010**, *39*, 1171. (b) Hashmi, A. S. K. *Catal. Today* **2007**, *122*, 211. (c) Wabnitz, T. C.; Yu, J.-Q.; Spencer, J. B. *Chem.—Eur. J.* **2004**, *10*, 484.
(16) Rosenfeld, D. C.; Shekhar, S.; Takemiya, A.; Utsunomiya, M.; Hartwig, J. F. *Org. Lett.* **2006**, *8*, 4179.
(17) Baik, M.-H.; Newcomb, M.; Friesner, R. A.; Lippard, S. J. *Chem. Rev.* **2003**, *103*, 2385.
(18) (a) Andreatta, J. R.; McKeown, B. A.; Gunnoe, T. B. *J. Organomet. Chem.* **2011**, *696*, 305. (b) McKeown, B. A.; Gonzalez, H. E.; Friedfeld, M. R.; Gunnoe, T. B.; Cundari, T. R.; Sabat, M. *J. Am. Chem. Soc.* **2011**, *133*, 19131. (c) McKeown, B. A.; Foley, N. A.; Lee, J. P.; Gunnoe, T. B. *Organometallics* **2008**, *27*, 4031. (d) Joslin, E. E.; McMullin, C. L.; Gunnoe, T. B.; Cundari, T. R.; Sabat, M.; Myers, W. H. *Organometallics* **2012**, *31*, 6851.
(19) Luedtke, A. T.; Goldberg, K. I. *Angew. Chem., Int. Ed.* **2008**, *47*, 7694.
(20) Bhalla, G.; Bischof, S. M.; Ganesh, S. K.; Liu, X. Y.; Jones, C. J.; Borzenko, A.; Tenn, W. J.; Ess, D. H.; Hashiguchi, B. G.; Lokare, K. S.; Leung, C. H.; Oxgaard, J.; Goddard, W. A.; Periana, R. A. *Green Chem.* **2011**, *13*, 69.
(21) (a) Pathak, T. P.; Osiak, J. G.; Vaden, R. M.; Welm, B. E.; Sigman, M. S. *Tetrahedron* **2012**, *68*, 5203. (b) Rozenman, M. M.; Kanan, M. W.; Liu, D. R. *J. Am. Chem. Soc.* **2007**, *129*, 14933. (c) Li, Z.; Zhang, J.; Brouwer, C.; Yang, C.-G.; Reich, N. W.; He, C. *Org. Lett.* **2006**, *8*, 4175. (d) Li, K.; Foresee, L. N.; Tunge, J. A. *J. Org. Chem.* **2005**, *70*, 2881. (e) Booth, B. L.; Al-Kinany, M.; Laali, K. *J. Chem. Soc., Perkin Trans. 1* **1987**, 2049.
(22) Wilcox, C. F.; Jesaitis, R. G. *J. Org. Chem.* **1968**, *33* (5), 2154.
(23) Adam, W.; Doerr, M.; Hill, K.; Peters, E. M.; Peters, K.; Von Schnering, H. G. *J. Org. Chem.* **1985**, *50*, 587.
(24) Coe, J. W.; Wirtz, M. C.; Bashore, C. G.; Candler, J. *Org. Lett.* **2004**, *6*, 1589.
(25) Procedure modernized from that of the following study: Wilcox, C. F.; Craig, R. R. *J. Am. Chem. Soc.* **1961**, *83*, 4258. The reagents were degassed, and 2,5-di-*tert*-butylhydroquinone was omitted.
(26) (a) Blank, F.; Janiak, C. *Coord. Chem. Rev.* **2009**, *253*, 827. (b) Kennedy, J. P.; Makowski, H. S. *J. Polym. Sci., Part C: Polym. Symp.* **1968**, *22*, 247. (c) Kennedy, J. P.; Makowski, H. S. *J. Macromol. Sci., Chem.* **1967**, *1*, 345.
(27) Antoniotti, S.; Dalla, V.; Duñach, E. *Angew. Chem., Int. Ed.* **2010**, *49*, 7860.
(28) Periana, R. A.; Bergman, R. G. *J. Am. Chem. Soc.* **1986**, *108*, 7346.
(29) van Koppen, P. A. M.; Bowers, M. T.; Fisher, E. R.; Armentrout, P. B. *J. Am. Chem. Soc.* **1994**, *116*, 3780.
(30) Nickon, A.; Kwasnik, H. R.; Mathew, C. T.; Swartz, T. D.; Williams, R. O.; DiGiorgio, J. B. *J. Org. Chem.* **1978**, *43*, 3904.
(31) Hill, G. S.; Irwin, M. J.; Levy, C. J.; Rendina, L. M.; Puddephatt, R. J. In *Inorganic Syntheses*; Darensbourg, M. Y., Ed.; Wiley: New York, 1998; Vol. 32, p 149.
(32) Rashidi, M.; Fakhroeian, Z.; Puddephatt, R. J. *J. Organomet. Chem.* **1990**, *406*, 261.
(33) Ong, C. M.; Jennings, M. C.; Puddephatt, R. J. *Can. J. Chem.* **2003**, *81*, 1196.
(34) Young, K. J. H.; Meier, S. K.; Gonzales, J. M.; Oxgaard, J.; Goddard, W. A.; Periana, R. A. *Organometallics* **2006**, *25*, 4734.
(35) Coughlin, D. J.; Salomon, R. G. *J. Org. Chem.* **1979**, *44*, 3784.
(36) Nigmatova, V. B.; Zaitsev, Y. V.; Anfilogova, S. N.; Pekhk, T. I.; Belikova, N. A. *Zh. Org. Khim.* **1994**, *30*, 686.
(37) Frisch, M. J.; Trucks, G. W.; Schlegel, H. B.; Scuseria, G. E.; Robb, M. A.; Cheeseman, J. R.; Scalmani, G.; Barone, V.; Mennucci, B.; Petersson, G. A.; Nakatsuji, H.; Caricato, M.; Li, X.; Hratchian, H. P.; Izmaylov, A. F.; Bloino, J.; Zheng, G.; Sonnenberg, J. L.; Hada, M.; Ehara, M.; Toyota, K.; Fukuda, R.; Hasegawa, J.; Ishida, M.; Nakajima, T.; Honda, Y.; Kitao, O.; Nakai, H.; Vreven, T.; Montgomery, J. A., Jr.; Peralta, J. E.; Ogliaro, F.; Bearpark, M.; Heyd, J. J.; Brothers, E.; Kudin, K. N.; Staroverov, V. N.; Kobayashi, R.; Normand, J.; Raghavachari, K.; Rendell, A.; Burant, J. C.; Iyengar, S. S.; Tomasi, J.; Cossi, M.; Rega, N.; Millam, J. M.; Klene, M.; Knox, J. E.; Cross, J. B.; Bakken, V.; Adamo, C.; Jaramillo, J.; Gomperts, R.; Stratmann, R. E.; Yazyev, O.; Austin, A. J.; Cammi, R.; Pomelli, C.; Ochterski, J. W.; Martin, R. L.; Morokuma, K.; Zakrzewski, V. G.; Voth, G. A.; Salvador, P.; Dannenberg, J. J.; Dapprich, S.; Daniels, A. D.; Farkas, O.; Foresman, J. B.; Ortiz, J. V.; Cioslowski, J.; Fox, D. J.; *Gaussian 09*, revision C.01; Gaussian Inc.: Wallingford, CT, 2010.